Earthquake Research Advances 5 (2025) 100389

Contents lists available at ScienceDirect

Earthquake Research Advances

journal homepage: www.keaipublishing.com/en/journals/earthquake-research-advances

Crustal velocity structure and composition of Bayan Har block and surrounding areas

Jiyan Lin [a], Tao Xu [b,*], Zhenyu Fan [a], Yong Qiu [a], Minjie Chen [a], Yonghong Duan [a]

[a] Geophysical Exploration Center, China Earthquake Administration, Zhengzhou, 450002, China
[b] Key Laboratory of Deep Petroleum Intelligent Exploration and Development, Institute of Geology and Geophysics, Chinese Academy of Sciences, Beijing, 100029, China

ARTICLE INFO

Keywords:
NE Qingzang plateau
Bayan Har
Crustal velocity structure
Crustal composition

ABSTRACT

The Bayan Har block, one of China's most seismically active regions, has experienced multiple major earthquakes ($\geq M$ 7.0) in recent years. It is a key area for investigating the interactions between the Qinghai-Xizang (Qingzang) Plateau and adjacent blocks, plateau uplift, and strong earthquake mechanisms. P-wave velocity and crustal composition provide key constraints on the properties of distinct tectonic units and their evolutionary modification processes. Based on the results of 8 Deep Seismic Sounding (DSS) profiles completed in the Bayan Har block and surrounding areas over the past 20 years, We constructed one-dimensional P-wave velocity models for the crust of Bayan Har block, Qilian fold belt, Qinling fold belt, Alxa block, Ordos block and Sichuan basin. Furthermore, crustal composition models for different tectonic units were established based on these results. The results reveal that the crustal thickness of the Bayan Har block gradually decreases towards the NNE, NE, and SE directions, while the average crustal velocity increases correspondingly. The felsic layer in the crust accounts for more than half of the total crustal thickness. The mafic content within the crust of different tectonic units exhibits notable variations, which may reflect that the Bayan Har block, Qilian fold belt, and Qinling fold belt have experienced more intensive lithospheric evolution processes compared to Ordos basin and Sichuan basin. The seismicity distribution in this region is significantly controlled by crustal velocity and composition heterogeneity across the Bayan Har block and adjacent areas, which demonstrates that earthquakes within and around the Bayan Har block exhibit both high frequency and larger magnitudes. These seismic characteristics primarily result from intense crustal stress accumulation and release during the outward expansion of the Qingzang Plateau.

1. Introduction

The Bayan Har block, located in the northeastern Qingzang Plateau, is a long, strip-like tectonic domain bounded by the Qilian fold belt, Qinling fold belt, Sichuan Basin, and the Qiangtang block (Fig. 1), which presents a shape of an inverted triangular, narrowing westward and widening eastward (Xu et al., 2008; Wen et al., 2011; Jia et al., 2017). The Bayan Har Block and its surrounding regions are among the most seismically active areas in China (Deng et al., 2010). Earthquakes of *M* 3.0 to *M* 6.9 occurred from January 2009 to August 2023, as well as major earthquakes of *M* 7.0 and above since 1970 have been collected (Fig. 1). Within the Bayan Har block and its periphery, 11 major earthquakes ($M \geq 7.0$) and 114 moderate to strong earthquakes ($M \geq 5.0$) have occurred. Notably, in recent years, several significant earthquakes have occurred and caused great damage, including the *M* 6.1 Lushan, *M* 6.0 Barkam, and *M* 6.8 Luding earthquakes (Li et al., 2022, 2024a; Xu and Guo, 2023). The distribution characteristics of great earthquakes ($M \geq 7.0$) indicate that the vast majority of these events occurred along the margins and within the interior of the Bayan Har block, indicating that the Bayan Har block plays a significant role in the uplift of Qingzang Plateau.

In recent years, a substantial amount of deep exploration work has been conducted in the Bayan Har block and its surrounding regions, and a wealth of research results has been obtained. Significant variations exist in the Moho depth and Moho nature among the Bayan Har block and its surrounding tectonic units. The crustal thickness decreases progressively from the southwest to the northeast. Specifically, the crustal thickness in the Qilian fold belt exceeds 60 km. In the western Qinling fold belt, the crust thins from west to east, with a variation range of 55 km–40 km. The crustal thicknesses of the Alxa and Ordos blocks are 50 km and 42 km,

* Corresponding author.
E-mail address: xutao@mail.iggcas.ac.cn (T. Xu).
Peer review under the responsibility of Editorial Board of Earthquake Research Advances.

https://doi.org/10.1016/j.eqrea.2025.100389
Received 18 October 2024; Received in revised form 6 April 2025; Accepted 11 April 2025

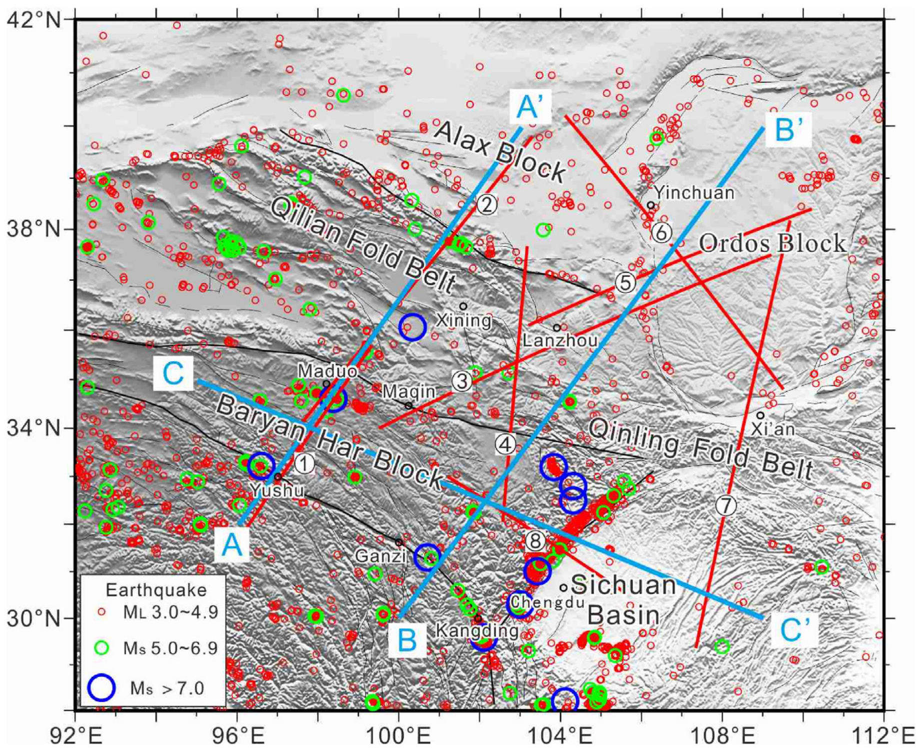

Fig. 1. Map showing geological structures, location of deep seismic sounding profiles and earthquake distribution. Deep seismic sounding profiles (Red solid lines): ① Leiwuqi-Wenquan (Zhang et al., 2014, Chinese); ② Maduo-Gonghe-Menyuan-Yabulai (Jia et al., 2019); ③ Dari-Lanzhou-Jingbian (Liu et al., 2006); ④ Barkam-Luqu-Gulang (Zhang et al., 2008, Chinese); ⑤ Lanzhou-Huianbu-Yulin (Wang et al., 2018b); ⑥ Tongchuan-Huanbu-Alax left banner (Wang et al., 2018b); ⑦ Yulin-Xianyang-Fuling (Teng et al., 2014, Chinese); ⑧ Suining-Mianzhu-Maoxian-Aba (Jia et al., 2014, Chinese). The time of the earthquakes (Hollow circles): M 3.0–6.9: 2009.01–2023.08; Magnitude greater than or equal to 7.0: 1970-present. The position of the light blue solid lines correspond to the vertical sections shown in Fig. 6.

respectively. Additionally, a distinct low-velocity zone is observed in the middle and lower crust of the Bayan Har block (Wang et al., 2017a, 2018a; Wu et al., 2017, 2023; Ma and Wu, 2025; Xu et al., 2014; Deng et al., 2015). The lithospheric thickness also exhibits significant variations. Specifically, the northeastern Bayan Har block and the western Qinling orogenic belt have relatively thin lithospheres, ranging from approximately 125 km to 135 km, while the southern Ordos block and the Alxa block exhibit thicker lithospheres, reaching 170–200 km (Chen et al., 2005; Zhang et al., 2013). Based on teleseismic P-wave tomography, low-velocity anomalies in the upper mantle have been identified, along with prominent high-velocity anomalies in the mantle transition zone. These results suggest that the interaction between the Qingzang Plateau and its surrounding blocks may extend to the upper mantle, providing evidence for lithospheric delamination (Guo et al., 2017). The middle and lower crust in the northeastern part of the Bayan Har block and the western segment of the Qinling fold belt exhibits relatively low velocity and Poisson's ratio, suggesting the absence of magma underplating. The dominant crustal composition is intermediate to felsic rocks, generally lacking of mafic material in the lower crust. These results further support the inference that the plastic material flow from the Qingzang Plateau towards the Qinling fold belt likely occurs beneath the lithosphere (Li et al., 2006, 2024b; Wang et al., 2017b; Ye et al., 2017; Wu et al., 2024). Frequency characteristics of receiver functions on either side of most fault zones of the Bayan Har block exhibit significant differences of the complexity and heterogeneity of Moho. Researchers proposed a new deep dynamic model based on the distinct double-layered crustal structure and high-velocity layers within the crust in the Yushu earthquake area. (Shen, 2013; Song et al., 2022). Additionally, deep seismic reflection profiles revealed detailed structures of the Bayan Har block and the Qinling orogenic belt. These studies identified northward-dipping reflectors in the lower crust and nearly flat Moho reflections, which are interpreted as indicative of the subduction of the Songpan block beneath the western Qinling and the subsequent strong extensional thinning of the crust (Gao et al., 2006; Wang et al., 2014, 2023). These deep exploration results provide a foundation for cognizing the uplift of the Qingzang Plateau and the evolution of the lithosphere. However, there are still debates regarding the uplift models of the plateau and the mechanisms of strong earthquakes.

Over the past 20 years, 8 DSS profiles have been completed in this region (Fig. 1). These profiles traverse the Bayan Har block, Qilian fold belt, Qinling fold belt, and other tectonic units from different directions, providing a foundation for further research on the contact relationships between these tectonic units, as well as the uplift of the Qingzang Plateau. In this paper, we construct one-dimensional crustal P-wave velocity models for these tectonic units by using the results from these DSS profiles. Based on these velocity models, we developed crustal composition models for each tectonic unit, and conducted an in-depth analysis of the discrepancy for each unit. Additionally, we integrate the seismic activity characteristics of the study area to explore the relationship between variations in crustal structure and seismic activity.

2. Method for constructing 1D P-wave velocity models of the crust

Different methods were used for constructing crustal velocity models based on the DSS data of various years (Fig. 1). For DSS profiles with available original waveform data, we use the method of horizontal layered seismic wave travel time calculations (Zhu et al., 1988) to construct 1D crustal P-wave velocity models, which include the Leiwuqi-Wenquan, Mado–Gonghe–Menyuan–Yabulai, Dari-Lanzhou-Jingbian, Barkam-Luqu-Gulang, and Suining-Mianzhu-Maoxian-Aba profiles. While other profiles without original data, we employ a model digitization method. This involves extracting P-wave velocity values at corresponding depths from published crustal P-wave velocity model diagrams to construct crustal P-wave velocity models. These profiles include the Lanzhou–Huianbu–Yulin, Tongchuan–Huianbu–Alashan left banner, and Yulin–Xianyang–Fuling profiles.

3. Crustal structure of Bayan Har block and surrounding areas

3.1. Bayan Har block

A DSS profile with a length of approximately 540 km across the Yushu M 7.1 earthquake area was conducted in 2010, and named the "Leiwuqi-

Wenquan" profile (Fig. 1). The research results indicate that the crustal thickness in the middle segment of the Bayan Har block is about 60 km, with an average crustal velocity of approximately 5.95–6.12 km/s, which is relatively low. The thickness of sedimentary cover is about 2.0–3.0 km, with velocities ranging from 3.2 to 5.0 km/s. The upper crust is approximately 15 km thick, with velocities of about 5.5–5.9 km/s. The middle crust is about 20 km thick, with velocities of 5.9–6.33 km/s. The lower crust is about 25 km thick, with velocities ranging from 6.3 to 6.85 km/s (Zhang et al., 2014; Jia et al., 2017). The crust exhibits a layered structure with alternating high and low velocity layers. The relatively thick crust, low average crustal velocity, and the layered velocity structure with alternating high and low velocity layers suggest that the middle segment of the Bayan Har block has experienced significant crustal reworking during the crustal thickening process of the Qingzang Plateau (Fig. 2).

Crustal structure for the eastern segment of the Bayan Har block has revealed by two DSS profiles named the "Barkam-Luqu-Gulang" and "Suining–Mianzhu–Maoxian–Aba" profiles (Zhang et al., 2008; Jia et al., 2014) (Fig. 1). The crustal thickness here is approximately 50 km–56 km, with an average crustal velocity of around 6.10 km/s. The sedimentary cover layer is about 2.5 km–3.0 km thick, with velocities ranging from 3.6 km/s to 5.1 km/s. The upper crust is approximately 17 km thick, with velocities of about 5.9–6.2 km/s. The middle crust is about 13 km thick, with velocities of 6.1 km/s–6.3 km/s. The lower crust is about 23 km thick, with velocities ranging from 6.3 km/s to 6.8 km/s (Zhang et al., 2008; Jia et al., 2014). The crust in this region also exhibits a distinct layered structure with alternating high and low velocity layers. Compared with the crustal structure of the middle segment of the Bayan Har block, the eastern segment shows crustal thinning of about 5 km–10 km. The velocities in the middle and lower crust are generally lower, while the upper crust velocities are relatively higher by approximately 0.3 km/s–0.4 km/s. This may indicate that the middle segment of the Bayan Har block has experienced stronger compressional forces than the eastern segment, leading to crustal thickening and a significant reduction in velocity (Fig. 2).

3.2. Qilian fold belt

The "Maduo–Gonghe–Menyuan–Yabulai" DSS profile (Guo et al., 2016; Jia et al., 2019) traverses the middle segment of the Qilian fold belt, providing valuable insights into its deep structure (Fig. 1). The sedimentary layer thickness is approximately 2–4 km, with velocities ranging from 3.5 to 4.6 km/s. The crust can be divided into three layers, with thicknesses of about 20 km each, and average velocities of approximately 5.95 km/s, 6.05 km/s, and 6.4 km/s, respectively. The crustal thickness is about 55–60 km, with an average crustal velocity of 5.96 km/s–6.05 km/s. The uppermost mantle has a relatively low velocity of about 7.75–7.95 km/s (Fig. 3). A large scale low-velocity anomaly exists in the upper crust of the Qilian fold belt, with velocities of approximately 5.8 km/s–5.9 km/s, which is 0.2 km/s–0.3 km/s lower than that of the Alxa block. Smaller scale low velocity anomalies are also detected in the middle and lower crust, indicating that the Qilian fold belt has undergone a certain degree of deformation during the orogenic compression process (Guo et al., 2016; Jia et al., 2019).

The DSS profiles “Dari–Lanzhou–Jingbian” and “Barkam-Luqu-Gulang” traverse the easternmost part of the Qilian fold belt (Liu et al., 2006; Zhang et al., 2008). The results indicate that the crustal thickness is approximately 48 km, significantly thinner than the middle segment of the Qilian fold belt by about 7 km–12 km. The crust exhibits a multi-layered structure with alternating high and low velocity layers. A distinct low-velocity anomaly is present within the depth range of 10 km–20 km, with velocity values of about 5.9 km/s, showing some similarity to the middle segment of the Qilian fold belt. The Longzhong Basin, located at the easternmost part of the Qilian fold belt, is separated from the eastern Ordos block by the Haiyuan fault. The crustal thickness of the Longzhong Basin is about 50 km, which is approximately 8 km thicker than that of the Ordos block. The average crustal velocity is relatively high, and there are no obvious low velocity zones within the crust, indicating a relatively stable structural characteristic. The crust can be divided into two layers at a depth of about 25 km, with the upper crust having velocities of 4.4–6.3 km/s and the lower crust having velocities of 6.45 km/s–6.8 km/s. Results from receiver functions show that there is no significant crustal deformation within the Longzhong Basin and the Ordos block. Crustal deformation is confined to a very narrow zone near the Liupanshan Mountain (Tian et al., 2021).

3.3. Qinling fold belt

The "Dari-Lanzhou-Jingbian", "Barkam-Luqu-Gulang" and "Yulin–Xianyang–Fuling" DSS profiles (Liu et al., 2006; Zhang et al., 2008; Teng et al., 2014) traverse the Qinling fold belt from different locations (Fig. 1). The crustal thickness of the Qinling fold belt is approximately 48–55 km, with significant thickening in the westernmost Maqin area. The average crustal velocity is about 6.3–6.4 km/s, with higher surface velocities at around 5.3 km/s–5.4 km/s. The crust exhibits a layered structure with alternating high and low velocity layers in the western part of the Qinling fold belt. In contrast, the eastern part has a simpler crustal structure, which can be divided into two layers. The upper

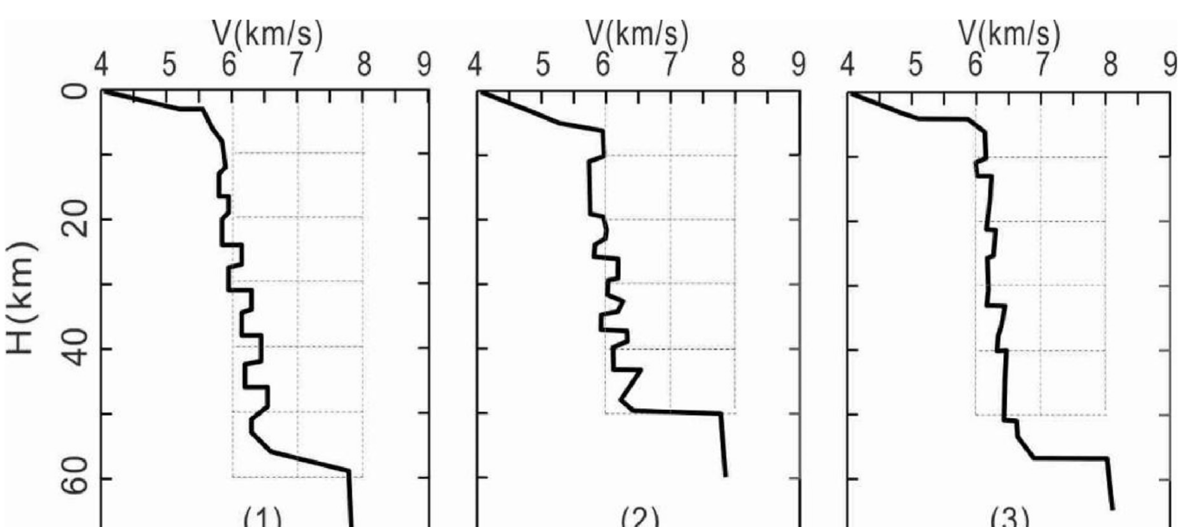

Fig. 2. Comparison of crustal P-wave velocity structure of varied areas in Bayan Har block. Location: see Fig. 5a.

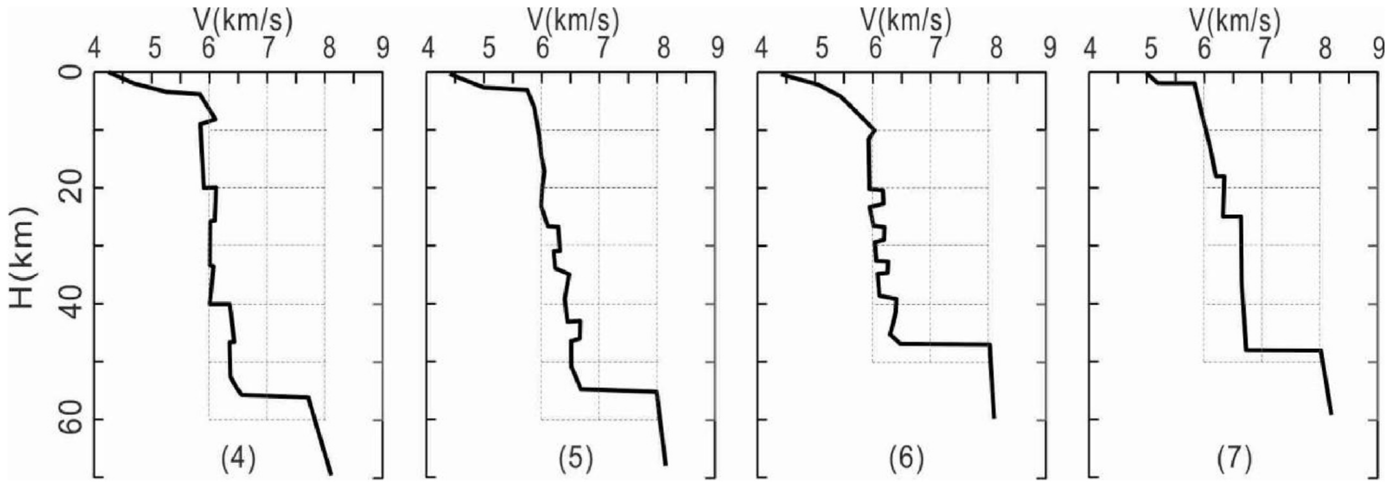

Fig. 3. Comparison of crustal P-wave velocity structure of varied areas in Qilian fold belt and Qinling fold belt. Location: (4) Qilian fold belt; (5–7) Qinling fold belt (Fig. 5a).

crust is about 26 km thick, with velocities ranging from 5.3 km/s to 6.30 km/s, while the lower crust is approximately 22 km thick, with velocities of 6.5 km/s–6.9 km/s. There are no obvious low velocity layers within the crust (Fig. 3). Compared with the Ordos block to the north and the Sichuan Basin to the south, the Qinling fold belt has a thicker crust by about 5 km–6 km. The upper crust shows higher velocity characteristics, and in most areas, bedrock is directly exposed at the surface.

3.4. Alxa block

The DSS profiles "Madoi–Gonghe–Menyuan–Yabulai" and "Tongchuan–Huianbu–Alxa left banner" (Jia et al., 2019; Wang et al., 2018b) extend into the Alxa block (Fig. 1), revealing similar crustal structural characteristics. The crystalline basement of the Alxa block is buried at a depth of approximately 2 km–4 km. The crust can be roughly divided into three layers: the upper crust, middle crust, and lower crust. The upper crust is about 13 km–16 km thick, with an average velocity of approximately 6.08 km/s. The middle crust is about 14 km–17 km thick, with an average velocity of approximately 6.26 km/s. The lower crust is about 12 km–14 km thick, with an average velocity of approximately 6.60 km/s. There are no obvious low velocity layers within the crust. The crustal thickness is about 46 km–50 km, with the eastern part of the Alxa block being slightly thicker than the western part. The average crustal velocity is approximately 6.28 km/s, and the uppermost mantle exhibits a relatively high of about 8.12 km/s, indicating a stable crustal structure (Fig. 4).

3.5. Ordos block

The "Yulin-Xianyang-Fuling", "Dari-Lanzhou-Jingbian" and "Lanzhou-Huianpu-Yulin" DSS profiles (Teng et al., 2014; Liu et al., 2006; Wang et al., 2018b) traverse the southern part of the Ordos block (Fig. 1). The crustal velocity structure reveals that the crystalline basement is buried at a depth of approximately 3 km–5 km, with sedimentary cover velocities ranging from 2 km/s to 5 km/s. The crustal thickness is about 40–42 km and can be divided into two layers: the upper crust, which is approximately 20–25 km thick with velocities of 6.0 km/s–6.3 km/s, and the lower crust, which is about 20 km–22 km thick with velocities of 6.5 km/s–6.9 km/s. No low velocity layers are detected within the crust, and the average crustal velocity is about 6.1 km/s–6.3 km/s. These characteristics reflect the weak internal deformation and relatively stable structural features of the Ordos block (Fig. 4).

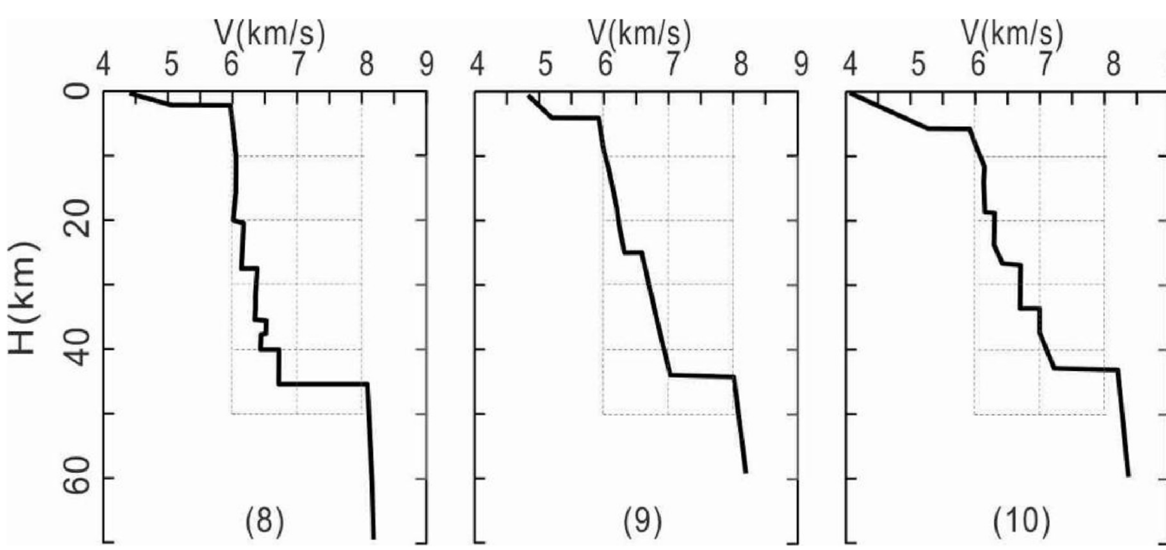

Fig. 4. Comparison of crustal P-wave velocity structure of varied areas in Alxa block, Ordos block and Sichuan basin. Location: (8) Alxa block; (9) Ordos block; (10) Sichuan basin (Fig. 5a).

3.6. Sichuan basin

The DSS profile "Yulin–Xianyang–Fuling" (Teng et al., 2014) is located in the eastern part of the Sichuan Basin (Fig. 1). The result indicates that the crustal thickness is approximately 43 km, with an average crustal velocity of 6.26 km/s. The sedimentary cover is about 2 km thick, with velocities ranging from 4.7 km/s to 5.4 km/s. The upper crust is about 26 km thick, with velocities of approximately 5.6 km/s–6.3 km/s, while the lower crust is about 17 km thick, with velocities ranging from 6.6 km/s to 7.0 km/s. The uppermost mantle has a relatively high velocity of about 8.0 km/s–8.3 km/s. The DSS profile "Suining–Mianzhu–Maoxian–Aba" (Jia et al., 2014) traverses the western part of the Sichuan Basin (Fig. 1). The velocity model shows that the crustal thickness is about 42 km, with an average crustal velocity of 6.15 km/s. The sedimentary cover is approximately 6 km thick, with velocities ranging from 3.6 km/s to 5.2 km/s. The uppermost mantle velocity is about 8.15 km/s–8.20 km/s. The crust is divided into three layers at depths of 12 km–16 km, 6 km–8 km, and 16 km–18 km, with corresponding velocities of 6.0 km/s–6.2 km/s, 6.3 km/s–6.4 km/s, and 6.6 km/s–7.2 km/s, respectively (Fig. 4).

The results from these two DSS profiles traversing different parts of the Sichuan basin show similar crustal velocity structures, reflecting uniform layered, weakly deformed, and stable cratonic crustal characteristics. These features also provide favorable tectonic conditions for the accumulation of oil and gas in the Sichuan basin.

4. Discussion

4.1. Velocity structure differences between the Bayan Har block and surrounding blocks

Significant variations in crustal structure are observed from the Alxa Block southwestward to the Yushu region. The Alxa block has a crustal thickness of approximately 46 km–50 km with an average crustal velocity of 6.28 km/s. In contrast, the middle segment of the Qilian fold belt to its southwest has a crustal thickness of about 60 km and an average crustal velocity of 5.95 km/s–6.05 km/s. Further to the southwest, the middle segment of the Bayan Har block (Yushu–Maduo region) also demonstrates a crustal thickness of about 60 km, with an average crustal velocity of 5.95 km/s–6.12 km/s. Compared to the stable Alxa block, the middle segments of both the Qilian fold belt and the Bayan Har block exhibit significant crustal thickening by approximately 10 km–14 km, accompanied by a reduction in average crustal velocity of 0.23 km/s–0.33 km/s. The crust in this region also displays distinct low-velocity anomalies and a multi-layered structure with alternating high and low velocity layers. Additionally, while the uppermost mantle velocity beneath the Alxa block is about 8.12 km/s, it decreases to about 7.75 km/s–7.95 km/s beneath the middle segments of the Qilian fold belt and the Bayan Har block, representing a reduction of 0.17 km/s–0.37 km/s. Compared to the relatively stable Alxa block, the middle segments of the Qilian fold belt and the Bayan Har block exhibit significant crustal thickening and notable reductions in average crustal velocity and uppermost mantle, which reflects substantial structural changes in the crust and uppermost mantle during the expansion of the Qingzang Plateau.

The eastern segment of the Bayan Har block has a crustal thickness of approximately 50 km–55 km and an average crustal velocity of about 6.10 km/s. The western segment of the Qinling fold belt and the eastern segment of the Qilian fold belt exhibit similar crustal structures, with a crustal thickness of about 48 km and an average crustal velocity of approximately 6.05 km/s. In the Longzhong basin area at the easternmost part of the Qilian fold belt, the crustal thickness is about 50 km, with an overall higher crustal velocity. The crustal layering changes from three layers in the middle segment of the Qilian fold belt to two layers, and there are no obvious low-velocity structural features within the crust. The Sichuan basin and the Ordos basin, both large sedimentary basins formed since the Mesozoic, exhibit similar crustal structure. The sedimentary cover is about 2 km–6 km thick, the crustal thickness is approximately 42 km–43 km, and the average crustal velocity is 6.2 km/s–6.3 km/s. The crust typically exhibits a two-layer division with positive velocity gradients and absence of low velocity layers, showing well-stratified characteristics typical of cratonic blocks. The P-wave velocity at the top of the uppermost mantle is relatively high, at about 8.0 km/s–8.3 km/s, indicating typical cratonic structural features. Comparative analysis reveals the eastern Bayan Har block has 8 km–13 km thicker crust and 0.1 km/s–0.2 km/s lower average velocities than the Ordos and Sichuan basins. The structural discrepancies between the eastern segment of the Bayan Har block and the surrounding blocks reflect the process of eastward flow of Qingzang Plateau material. The material encounters resistance from the rigid Sichuan basin and Ordos block, leading to accumulation at the tectonic junctions. Particularly in the junction area between the Bayan Har block and the Sichuan basin, significant vertical deformation features are observed. The crust is significantly thickened, and the P-wave velocity is markedly reduced. The crust and the upper mantle material have experienced substantial changes.

4.2. Crustal composition differences between the Bayan Har block and surrounding blocks

In 1995 and 1996, Christensen and Mooney analyzed 560 global continental crustal samples, combined with petrophysical experimental data, and established a correlation between P-wave velocities and lithology (Christensen and Mooney, 1995; Christensen, 1996). Their work provides a basis for inferring crustal composition using crustal P-wave velocity. Based on the tectonic divisions in the study area, the composition of each tectonic unit is inferred from the velocity models (Fig. 5). The crustal composition classified into four layers: sedimentary cover ($Vp \leq 5.7$ km/s), felsic layer ($5.7 < Vp \leq 6.4$ km/s), intermediate layer ($6.4 < Vp \leq 6.9$ km/s), and mafic layer ($6.9 < Vp \leq 7.3$ km/s).

In terms of crustal thickness, the Bayan Har block has the thickest crust, reaching up to 60 km. The Qilian fold belt and the Qinling fold belt have intermediate crustal thicknesses, approximately 50 km–55 km. In contrast, the Alxa block, Ordos block, and Sichuan basin have the thinnest crust, averaging 42 km–45 km. In terms of sedimentary cover thickness, the Qilian fold belt and Qinling fold belt exhibit relatively thin sedimentary covers, with crystalline basement even directly outcropping at the surface in some areas. The Bayan Har block is primarily covered by Triassic and Permian rock formations, with a sedimentary thickness of 2 km–5 km. In contrast, the Alxa block, Ordos block and Sichuan basin possess relatively thicker sedimentary covers, with the Sichuan basin reaching 5 km–6 km and being overlain by Jurassic and Cretaceous strata at the surface. Regarding the thickness of felsic, intermediate, and mafic layers, the felsic layer occupies the largest proportion of the crust, followed by the intermediate rock layer, with the mafic layer being the smallest. In the Bayan Har block, Qilian fold belt, and Qinling fold belt, the thickness of the felsic layer is approximately 30 km–40 km, while the intermediate layer is about 10 km–15 km thick, with mafic layer generally being absent. According to petrophysical experimental data, lithology and velocity are also influenced by subsurface temperature. Based on the latest edition of the national database of heat flow (Wang et al., 2024), there is no direct evidence to prove that the crustal temperature of the Bayan Har block is significantly higher than surrounding tectonic units. Therefore, we speculate that the low crustal velocity of the Bayan Har block is attributed to variations of crustal lithology. A DSS profile, approximately 1600 km long, that traverses multiple tectonic units along the northeastern margin of the Qingzang Plateau, revealed that several tectonic units, including the southern Qilian mountains, the eastern Kunlun mountains, and the Songpan-Ganzi block, may lack mafic lower crust (Wang et al., 2013). Additionally, another DSS profile "Gamba–Xietongmen–Shenzha" similarly found no evidence of mafic layer in the central Qingzang Plateau (Wang et al., 2021). These two profiles provide crucial insights into the lower crustal structure of the study area and provide important evidence for inferring that the absence

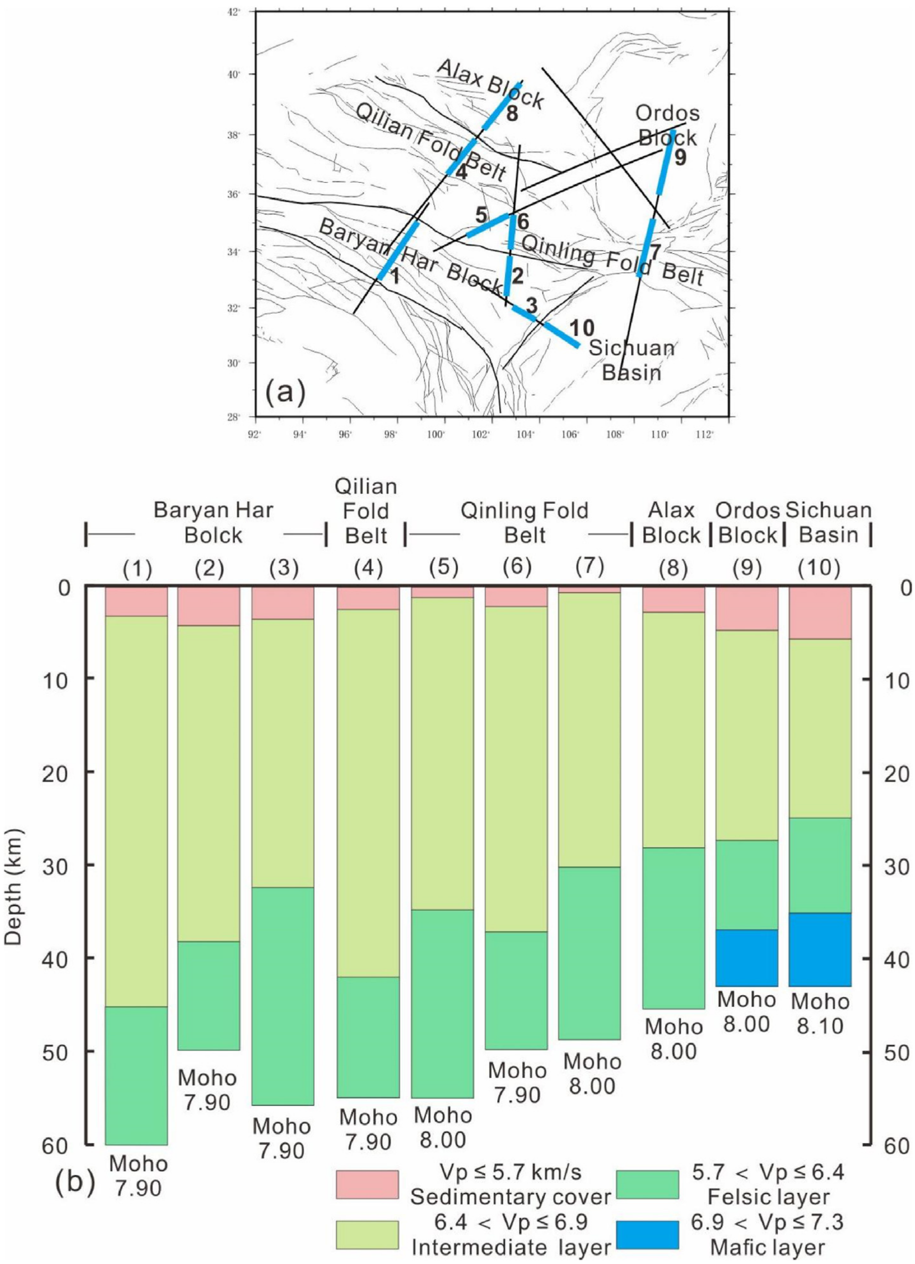

Fig. 5. Crustal composition of different tectonic units. (a) Locations of each model; (b) Crustal composition, Numbers with round brackets correspond to fig.(a).

of mafic layer may represent a regional scale phenomenon. Our research results indicate that the Ordos basin and the Sichuan basin contain a 5–8 km thick mafic layer within crust (Fig. 5), with the uppermost mantle exhibits relatively high P-wave velocities (8.0–8.1 km/s). These features demonstrate well-preserved cratonic basin features. Previous teleseismic receiver functions studies have shown that the Ordos basin has a lithospheric thickness of approximately 160–200 km, while the lithosphere-asthenosphere boundary beneath the Sichuan basin reaches depth of up to 190 km. These results indicate the preservation of a relatively thick lithospheric mantle root beneath these basins, maintaining the fundamental characteristics of cratonic stability (Chen et al., 2014; Zhang et al., 2018). Therefore, the preservation of mafic layers at the base of the crust in the Ordos and Sichuan basins may be attributed to the lack of large scale lithospheric modification. Notably, no mafic layer has been detected beneath the Alxa block, suggesting that the lower crust or lithosphere may have experienced certain degrees of modification. This alteration may have reduced the lower crustal velocities to below 6.9 km/s and caused a depletion of mafic material.

4.3. The relationship between seismic activity and crustal structure of the Bayan Har block and surrounding areas

To explore the relationship between seismic activity and crustal structure in the Bayan Har block and surrounding areas, we conducted cross-sections across different regions of the block (Fig. 1), including the NE-trending AA' and BB' profiles and the NW-trending CC' profile. Earthquakes within 100 km on either side of each profile were projected onto the corresponding sections, along with representative crustal velocity models and compositions of each tectonic unit. The NE-trending AA' profile crosses the Bayan Har block, the Qinling mountains, the Qilian fold belt, and the Alxa block. The crustal thickness decreases from 60 km in the Bayan Har block to approximately 46 km in the Alxa block. From the perspective of crustal heterogeneity, the Bayan Har block exhibits more dramatic velocity changes compared to the Qinling

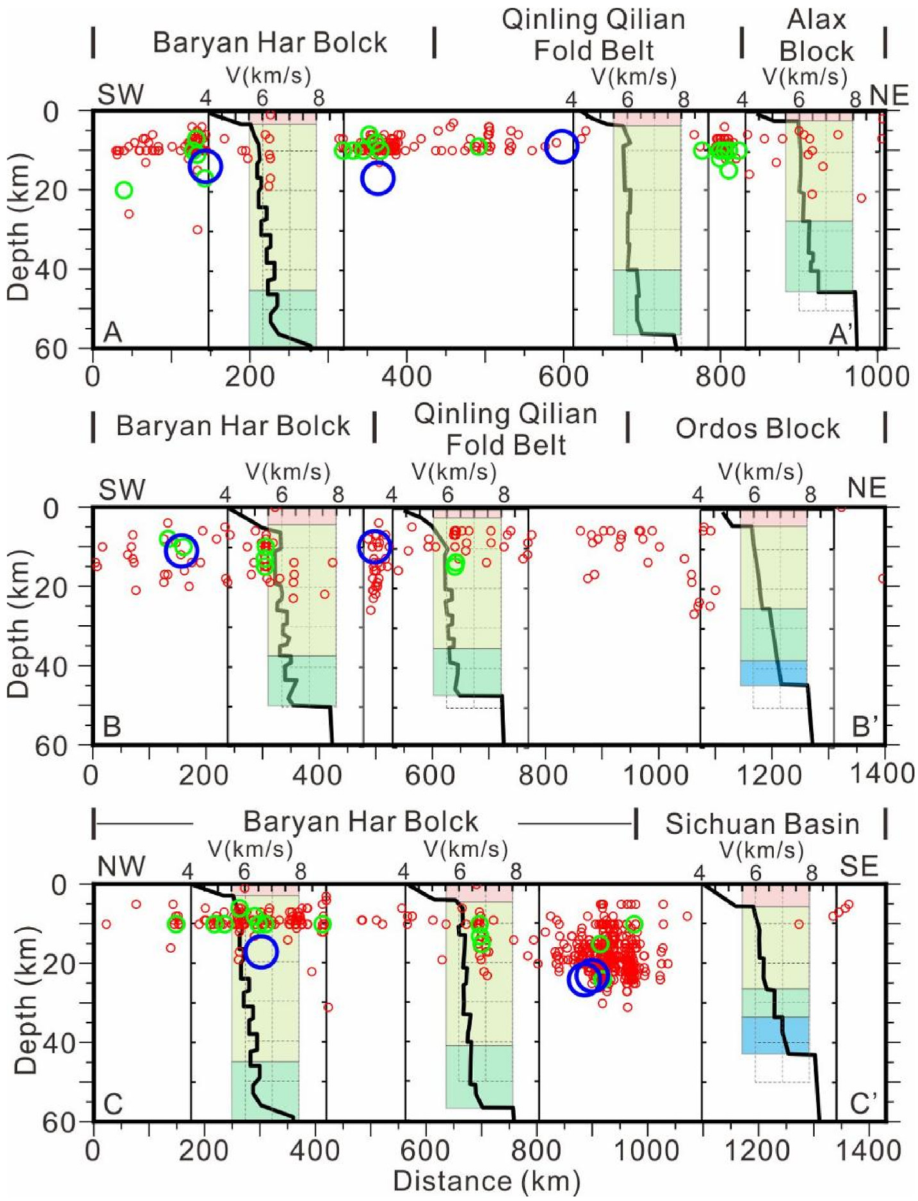

Fig. 6. Comparison of crustal structure of different tectonic units and earthquakes distribution. Locations of vertical sections correspond to light blue solid lines in Fig. 1. Hollow circles represent the projection of earthquakes within 100 km beside the profile, while red hollow circles show the magnitude of the earthquakes is 3.0–4.9, green hollow circles is 5.0–6.9, and blue hollow circles greater than 7.0. The time of the earthquakes (Hollow circles): Magnitude 3.0–6.9: 2009.01–2023.08; Magnitude greater than or equal to 7.0: 1970-present (Seismic database: https://news.ceic.ac.cn/index.html).

mountains and the Qilian fold belt, with distinct alternating high and low velocity layers within the crust. In contrast, the Alxa block lacks such characteristics. This likely reflects the intense crustal deformation experienced by the Bayan Har block as it encountered the rigid Alxa block during the northeastward extrusion of the Qingzang Plateau. This process resulted in reduced upper crustal velocities and the appearance of alternating high and low velocity layers. The earthquakes distribution map (Fig. 6) also shows that the Bayan Har block has significantly stronger seismic activity and larger earthquake magnitude compared to the Alxa block. This demonstrates that the Bayan Har block continuously releases the enormous energy accumulated from block compression through earthquakes during its deformation process.

The NE-trending BB' profile (Fig. 6) crosses the Bayan Har block, the Qinling mountains, the Qilian fold belt, and the Ordos block from southwest to northeast, exhibiting similar characteristics to the AA' profile. The crustal thickness decreases from 50 km in the Bayan Har block to approximately 42 km in the Ordos block. Seismic activity is mainly concentrated within the felsic upper crust, with moderate earthquakes occur within the Bayan Har block, the Qinling fold belt and Qilian fold belt. Strong earthquakes with magnitudes above 7 are located along the boundaries of the Bayan Har block, while almost no earthquakes occur within the Ordos block, which is consistent with its stable crustal structure and the presence of a mafic lower crust. The NW-trending CC' profile (Fig. 6) traverses the Bayan Har block and the Ordos block from northwest to southeast. The relatively concentrated seismic activity in these two tectonic units reflects the massive energy release process resulting from the Bayan Har block's compression toward the Sichuan Basin. The substantial differences in crustal thickness, middle and lower crustal structure, and composition between the Bayan Har block and the Ordos block indicate that the southeast boundary of the Bayan Har block has experienced more intense deformation. In contrast, to the northeast of the Bayan Har block, the presence of the Qilian and Qinling fold belts between the relatively stable Alxa block and Ordos block acts as a buffer zone to some extent, with the crustal structure showing gradual transitional characteristics.

5. Conclusions

(1) The Bayan Har block and its surrounding areas exhibit significant variations in crustal thickness and P-wave velocity. Crustal

thickness decreases gradually from about 60 km within the Bayan Har block to 46 km–50 km in the Alxa block, 40 km–42 km in the Ordos block, and about 43 km in the Sichuan basin. Correspondingly, the average crustal velocity increases from 5.95 to 6.12 km/s within the Bayan Har block to about 6.28 km/s in the Alxa block, about 6.1 km/s–6.3 km/s in the Ordos block, and 6.15 km/s –6.26 km/s in the Sichuan basin.

(2) The felsic layer in the Bayan Har block, Qilian fold belt, and Qinling fold belt likely accounts for more than half of the total crustal thickness. In contrast, the Ordos block and the Sichuan basin have a distinct mafic lower crust. This indicates that the lower crust of the Bayan Har block, Qilian fold belt, and Qinling fold belt has been significantly modified, while the Ordos block and the Sichuan Basin retain stable cratonic structural characteristics.

(3) The discrepancies in crustal structure and composition among these tectonic units are crucial factors contributing to the concentration of moderate to strong earthquakes in the Bayan Har block, Qilian fold belt, and Qinling fold belt, while seismic activity is rare in the Alxa block, Ordos block, and Sichuan basin.

CRediT authorship contribution statement

Jiyan Lin: Writing – original draft, Data curation. **Tao Xu:** Writing – review & editing, Supervision. **Zhenyu Fan:** Writing – original draft, Investigation, Data curation. **Yong Qiu:** Writing – original draft, Software. **Minjie Chen:** Writing – original draft, Investigation. **Yonghong Duan:** Writing – review & editing.

Declaration of competing interest

The authors declare that they have no known competing financial interests or personal relationships that could have appeared to influence the work reported in this paper. The corresponding author Tao Xu is an editorial board member of Earthquake Research Advances and not involved by the peer review process.

Author agreement and acknowledgement

I would like to declare on behalf of my co-authors that the work described was original research that has not been published previouslyand is not under consideration for publication elsewhere, that has not been published previously, and is not under consideration for publication elsewhere, in whole or in part. All the authors listed have approved the manuscript that is enclosed.

This work is supported by the National Key R&D Program of China (No. 2023YFC3012002), the National Natural Science Foundation of China (42374073).

References

Chen, J., Liu, Q., Li, S., Guo, B., Lai, Y., 2005. Crust and upper mantle S-wave velocity structure across Northeastern Tibetan Plateau and Ordos block. Chin. J. Geophys. 48 (2), 333–342 (in Chinese).
Chen, L., Jiang, M., Yang, J., Wei, Z., Liu, C., Ling, Y., 2014. Presence of an intralithospheric discontinuity in the central and western North China Craton: implications for destruction of the craton. Geology 42 (3), 223–226.
Christensen, N.I., 1996. Poisson's ratio and crustal seismology. J. Geophys. Res. 101 (B2), 3139–3156.
Christensen, N.I., Mooney, W.D., 1995. Seismic velocity structure and composition of the continental crust: a global view. J. Geophys. Res. 100 (B7), 9761–9788.
Deng, Q., Gao, X., Chen, G., Yang, H., 2010. Recent tectonic activity of Bayankala fault·block and the Kunlun-Wenchuan earthquake series of the Tibetan Plateau. Earth Sci. Front. 17 (5), 163–178 (in Chinese).
Deng, Y., Shen, W., Xu, T., Ritzwoller, M., 2015. Crustal layering in northeastern Tibet: a case study based on joint inversion of receiver functions and surface wave dispersion. Geophys. J. Int. 203, 692–706.
Gao, R., Ma, Y., Li, Q., Zhu, X., Zhang, J., Wang, H., Li, P., Lu, Z., Guan, Y., 2006. Structure of the lower crust beneath the Songpan block and West Qinling orogen and their relation as revealed by deep seismic reflection profiling. Geol. Bull. China 25 (12), 1361–1367 (in Chinese).
Guo, H., Ding, Z., Xu, X., 2017. Upper mantle structure beneath the northern South-North Seismic Zone from teleseismic traveltime data. Chin. J. Geophys. 60 (1), 86–97 (in Chinese).
Guo, W., Jia, S., Duan, Y., Wang, F., 2016. A study on the basement tectonic units in the northeast margin of Tibetan plateau-the result of Maduo-Gonghe-Yabrai refraction profile. Chin. J. Geophys. 59 (10), 3627–3636 (in Chinese).
Jia, S., Guo, W., Mooney, W.D., et al., 2019. Crustal structure of the middle segment of the Qilian fold belt and the coupling mechanism of its associated basin and range system. Tectonophysics 770, 128154.
Jia, S., Lin, J., Guo, W., Zhao, N., Qiu, Y., 2017. Investigation on diversity of crustal structure beneath Bayan Har block. Chin. J. Geophys. 60 (6), 2226–2238 (in Chinese).
Jia, S., Liu, B., Xu, Z., Liu, Z., Feng, S., Zhang, J., Lin, J., Tian, X., Liu, Q., Guo, W., 2014. The crustal structures of the central Longmenshan along and its margins as related to the seismotectonics of the 2008 Wenchuan Earthquake. Sci. China Earth Sci. 57, 777–790 (in Chinese).
Li, C., Sun, K., Ma, J., Li, J., Liang, M., Fang, L., 2022. The 2022 M6.8 Luding earthquake: a complicated event by faulting of the Moxi segment of the Xianshuihe fault zone. Seismol. Geol. 44 (6), 1648–1666 (in Chinese).
Li, J., Wu, Z., Su, J., Zou, K., Li, P., 2024a. Study of focal mechanism and aftershocks of the MS6.1 earthquake in Lushan on June 1th, 2022. Prog. Geophys. 39 (4), 1315–1329 (in Chinese).
Li, X., Li, S., Gao, Y., Xia, X., 2024b. Advancements in deep tectonics and dynamic mechanisms beneath the eastern Tibetan Plateau—inspirations from the 9th and 10th WTGTP Workshops. Rev. Geophys. Planet. Phys. 55 (2), 205–216 (in Chinese).
Li, Y., Wu, Q., An, Z., Tian, X., Zeng, R., Zhang, R., Li, H., 2006. The Poisson ratio and crustal structure across the NE Tibetan Plateau determined from receiver functions. Chin. J. Geophys. 49 (5), 1359–1368 (in Chinese).
Liu, M., Mooney, W.D., Li, S., et al., 2006. Crustal structure of the northeastern margin of the Tibetan plateau from the Songpan-Ganzi terrane to the Ordos basin. Tectonophysics 420, 253–266.
Ma, X., Wu, Q., 2025. Preliminary study on Moho reflection wave based on noise interference method and its application in crustal structure imaging of the northeastern margin of the Qinghai–Xizang Plateau. Rev. Geophys. Planet. Phys. 56 (2), 167–181 (in Chinese).
Shen, X., 2013. Imaging structures of crust and upper mantle beneath the source of the 14 April 2010 Yushu, Qinghai earthquake using P- and S- wave receiver functions. Chin. J. Geophys. 56 (2), 495–503 (in Chinese).
Song, T., Shen, X., Mei, X., Jiao, Y., Li, M., Su, X., Ji, W., 2022. Constraining Moho characteristics in the north-eastern margin of Tibet plateau with frequency-dependence of receiver function. Seismol. Geol. 44 (5), 1290–1312 (in Chinese).
Teng, J., Li, S., Zhang, Y., Wang, F., Pi, J., Zhao, J., Zhang, C., Qiao, Y., Hu, G., Yan, Y., 2014. Fine velocity structures and deep processes in crust and mantle of the Qinling orogenic belt and the adjacent North China craton and Yangtze craton. Chin. J. Geophys. 57 (10), 3154–3175 (in Chinese).
Tian, X., Bai, Z., Klemperer, S.L., et al., 2021. Crustal-scale wedge tectonics at the narrow boundary between the Tibetan Plateau and Ordos block. Earth Planet Sci. Lett. 554, 116700.
Wang, G., Lu, Z., Li, W., Wang, H., Cheng, Y., Chen, S., Cai, W., 2023. Development status of deep seismic reflection profile detection technology. Rev. Geophys. Planet. Phys. 54 (2), 120–139 (in Chinese).
Wang, G., Thybo, H., Artemieva, I.M., 2021. No mafic layer in 80 km thick Tibetan crust. Nat. Commun. 12 (1), 1069.
Wang, H., Gao, R., Li, Q., Li, W., Hou, H., Kuang, C., Xue, A., Huang, W., 2014. Deep seismic reflection profiling in the Songpan-west Qinling-Linxia basin of the Qinghai-Tibet plateau:data acquisition, data processing and preliminary interpretations. Chin. J. Geophys. 57 (5), 1451–1461 (in Chinese).
Wang, S., Liu, B., Tian, X., et al., 2018b. Crustal P-wave velocity structure in the northeastern margin of the Qinghai-Tibetan Plateau and insights into crustal deformation. Sci. China Earth Sci. 61, 1221–1237.
Wang, W., Wu, J., Fang, L., Lai, G., Cai, Y., 2017b. Sedimentary and crustal thicknesses and Poisson's ratios for the NE Tibetan Plateau and its adjacent regions based on dense seismic arrays. Earth Planet Sci. Lett. 462, 76–85.
Wang, X., Ding, Z., Wu, Y., Zhu, L., 2017a. Crustal thicknesses and Poisson's ratios beneath the northern section of the north-south seismic belt and surrounding areas in China. Chin. J. Geophys. 60 (6), 2080–2090 (in Chinese).
Wang, Y., Liu, S., Chen, C., Jiang, G., Wu, J., Guo, L., Wang, Y., Zhang, H., Wang, Z., Jiang, X., Zhu, C., Zuo, Y., Hu, J., Zhang, C., He, L., Hu, S., Pang, Z., Wang, J., 2024. Compilation of terrestrial heat flow data in continental China (5th edition). Chin. J. Geophys. 67 (11), 4233–4265 (in Chinese).
Wang, X., Chen, L., Ai, Y., Xu, T., Jiang, M., Ling, Y., 2018a. Crustal structure and deformation beneath eastern and northern Tibet revealed by P-wave receiver functions. Earth Planet Sci. Lett. 497, 69–79.
Wang, Y., Mooney, W.D., Yuan, X., Okaya, N., 2013. Crustal structure of the northeastern Tibetan Plateau from the southern Tarim basin to Sichuan basin, China. Tectonophysics 584, 191–208.
Wen, X., Du, F., Zhang, P., Long, F., 2011. Correlation of major earthquake sequences on the northern and eastern boundaries of the Bayan Har block, and its relation to the 2008 Wenchuan earthquake. Chin. J. Geophys. 54 (3), 706–716 (in Chinese).
Wu, G., Xiong, X., Gao, R., Chen, X., Li, Y., Wang, G., Ren, H., 2023. Moho depth of the Qilian orogen revealed by wide-angle reflection/refraction profiles. Rev. Geophys. Planet. Phys. 54 (2), 109–119 (in Chinese).

Wu, C., Xu, T., Tian, X., Mitchell, R.N., Lin, J., Yang, J., et al., 2024. Underthrusting of Tarim lower crust beneath the Tibetan Plateau revealed by receiver function imaging. Geophys. Res. Lett. 51, e2024GL108220.

Wu, Z., Xu, T., Badal, J., Yao, H., Wu, C., Zhang, Z., Teng, J., 2017. Crustal shear-wave velocity structure of northeastern Tibet revealed by ambient seismic noise and receiver functions. Gondwana Res. 41, 400–410.

Xu, X., Wen, X., Chen, G., Yu, G., 2008. Discovery of the Longriba fault zone in eastern Bayan Har block, China and its tectonic implication. Sci. China Earth Sci. 51, 1209–1223.

Xu, Y., Guo, X., 2023. Relocation of the 2022 Ms6.0 Maerkang earthquake swarm in Sichuan province and its seismic fault analysis. Seismol. Geol. 45 (4), 1006–1024 (in Chinese).

Xu, T., Wu, Z., Zhang, Z., Tian, X., Deng, Y., Wu, C., Teng, J., 2014. Crustal structure across the Kunlun fault from passive source seismic profiling in east Tibet. Tectonophysics 627, 98–107.

Ye, Z., Li, J., Gao, R., Song, X., Li, Q., Li, Y., Li, W., 2017. Crustal and uppermost mantle structure across the TibetQinling transition zone in NE Tibet: implications for material extrusion beneath the Tibetan Plateau. Geophys. Res. Lett. 44, 10316–10323.

Zhang, H., Teng, J., Tian, X., Zhang, Z., Gao, R., 2013. Lithospheric thickness and upper mantle anisotropy beneath the northeastern Tibetan Plateau. Chin. J. Geophys. 56 (2), 459–471 (in Chinese).

Zhang, J., Wang, F., Liu, B., Wang, S., Zhao, J., Zhang, C., Li, Y., Liu, Q., Liu, L., 2014. A study of the crust-mantle velocity structure beneath the Yushu earthquake zone and its adjacent areas. Seismol. Geol. 36 (2), 322–332 (in Chinese).

Zhang, X., Jia, S., Zhao, J., Zhang, C., Yang, J., Wang, F., Zhang, J., Liu, B., Sun, G., Pan, S., 2008. Crustal structures beneath West Qinling-East Kunlun orogen and its adjacent area-Results of wide-angle seismic reflection and refraction experiment. Chin. J. Geophys. 51 (2), 439–450 (in Chinese).

Zhang, Y., Chen, L., Ai, Y., Jiang, M., Xu, W., Shen, Z., 2018. Lithospheric structure of the south China block from S-receiver function. Chin. J. Geophys. 61 (1), 138–149 (in Chinese).

Zhu, J., Liu, F., Wang, C., Lu, H., Luo, X., 1988. Seismic Body Wave Calculation Method for Studying the Structure of Crust and Upper Mantle. China Science Publishing & Media Ltd., pp. 1–14 (in Chinese).